



Chemical Composition of Particulate Matter from Traffic Emissions in a Road Tunnel in Xi'an, China

Yanzhao Hao¹, Shunxi Deng^{2,4*}, Yan Yang^{3,4}, Wenbin Song⁵, Hui Tong⁴, Zhaowen Qiu¹

¹ School of Automobile, Chang'an University, Xi'an 710064, China

² Key Laboratory of Subsurface Hydrology and Ecological Effect in Arid Region of Ministry of Education, Chang'an University, Xi'an 710064, China

³ Chinese Research Academy of Environmental Sciences, Beijing 100012, China

⁴ School of Environmental Science and Engineering, Chang'an University, Xi'an 710064, China

⁵ Xi'an Environmental Protection Bureau, Xi'an 710054, China

ABSTRACT

Chemical compositions of particulate matter (PM) from traffic emissions vary by region and with time. Therefore, it is necessary to obtain local mobile source profiles of PM to support regional researches for vehicle emission control policy, source apportionment modeling, etc. In this study, PM_{2.5} and PM₁₀ samples were collected from a highway tunnel in Xi'an in northwestern China. The chemical composition, specifically, the OC, EC, water-soluble ions, and elements, was analyzed in detail to (1) provide local PM profiles for a mixed vehicle fleet, (2) identify the origins of different elements in the tunnel environment, and (3) determine the associated factors influencing the profiles. The PM_{2.5} profiles in the tunnel were identified as OC (34.10%), EC (11.96%), water-soluble ions (18.22%), and elements (27.73%), while the PM₁₀ profiles included OC (28.48%), EC (8.59%), water-soluble ions (14.17%), and elements (33.36%), respectively. The origins of the elements in the tunnel were classified into three categories by the receptor modeling approach: resuspended road dust and brake wear, vehicle exhaust and tire wear, and tailpipe emissions from diesel vehicles (DV). The mass fractions of OC, EC, and elements originating from resuspended road dust and brake wear were mainly affected by vehicle driving conditions (i.e., uphill/downhill and speed), whereas the mass content of bromine (Br) was influenced by the proportion of DV in the fleet.

Keywords: Traffic emissions; PM_{2.5}; PM₁₀; Source profile; Road tunnel.

INTRODUCTION

Particulate matter (PM) is a primary pollutant of atmospheric haze pollution in China, which has an adverse impact on public health, especially on human lungs and hearts (Delfino *et al.*, 2008; Spira-Cohen *et al.*, 2011; Liu *et al.*, 2015a). Motor vehicles are a major source of PM in the atmosphere. According to the official source apportionment results of PM_{2.5} in 15 cities of China (MEPC, 2018), the contribution of motor vehicles in 11 cities was greater than 20%, with an average value of 23.36%. In order to better control PM pollution, it is essential to understand the physical and chemical characteristics of the PM emitted from motor vehicles. Vehicle emissions can be investigated using various testing methods, such as the tunnel test (Pio *et al.*, 2013;

Alves *et al.*, 2015b), dynamometer test (Na *et al.*, 2015; Pietikainen *et al.*, 2015), and on-road test (Yao *et al.*, 2015; Zhang *et al.*, 2015a). Compared with other approaches, tunnel test can easily obtain the emission characteristics of PM with mixed vehicle fleet under actual driving conditions (Franco *et al.*, 2013; Pant *et al.*, 2017). Further, PM pollutants collected in the tunnel include not only vehicle exhaust, but also some associated emissions, such as friction emissions (tire, brake, and road surface wear) and road dust (Handler *et al.*, 2008; Thorpe and Harrison, 2008). Therefore, tunnel test can estimate the PM pollution caused by motor vehicles more comprehensively.

Faced with the increasingly serious air pollution problem, several studies have been conducted on the chemical characteristics of PM from vehicle emissions by means of tunnel tests in China. Most of these studies were carried out in the eastern part of China, mainly in Guangzhou (Huang *et al.*, 2006; He *et al.*, 2008; Dai *et al.*, 2015; Zhang *et al.*, 2015b), Hong Kong (Chiang and Huang, 2009; Ho *et al.*, 2009; Cheng *et al.*, 2010), and Shanghai (Zhao *et al.*, 2010; Liu *et al.*, 2015b, c). However, no such studies have

* Corresponding author.

Tel./Fax: + 86 29 82334207

E-mail address: dengshunxi@aliyun.com

been conducted in the western part of China, such as Xi'an, which is the capital of Shaanxi Province (Fig. 1). Xi'an is the largest city in northwestern China, with up to 2.42 million licensed vehicles in 2015. Moreover, vehicle emission was the second largest source of PM_{2.5} pollution in Xi'an, with contributions of 14.9% and 12.9% in urban and rural areas, respectively (Wang *et al.*, 2015). Considering that each region has its own characteristic vehicular fleet (vehicle type, fuel quality, etc.) and corresponding conditions (transportation infrastructure, driving conditions, etc.) that influence vehicular emissions, it is important to conduct local studies to obtain local emission profiles (Zhang *et al.*, 2015b; Alves *et al.*, 2016).

This study carried out a tunnel experiment in Xi'an, with the following objectives: (1) investigate the chemical characteristics of PM in a typical highway tunnel, and obtain the local mobile source profiles of PM; (2) identify the main sources of each element in PM, such as vehicle exhaust, tire wear, brake wear, and resuspended road dust; and (3) determine the main factors affecting the chemical composition of PM from road traffic. Results from this study will provide necessary data for subsequent studies in northwestern China, such as vehicle emission control policy, source apportionment modeling, and air quality simulation.

MATERIALS AND METHODOLOGY

Sampling Sites

The sampling experiment was conducted in the Qinling No. 1 Tunnel, which is located in the southwest suburb of Xi'an. There are no significant anthropogenic pollution sources around it, apart from motor vehicles. This highway tunnel has two independent bores (southbound and northbound), each of which has two lanes, as shown in Fig. 1. The southbound bore is 6102 m in length, with an upgrade of +2.58% (uphill); whereas the northbound bore is 6144 m, with a downgrade of -2.58% (downhill). A ventilation shaft was placed at 1657 m from the entrance of the northbound bore, which was ventilated naturally during the test. There were four sampling sites in the southbound bore, with three sampling sites in the northbound bore (Fig. 1). More details of the sampling sites are summarized in Section A1 in the supplementary material. The samplers were placed in the emergency parking areas at a distance of 3 m from the nearside lane. This experiment was performed for several purposes, such as determining gas pollution (e.g., CO, NO_x, SO₂, and O₃) and visibility in the tunnel, while this study only focused on the chemical composition of the PM.

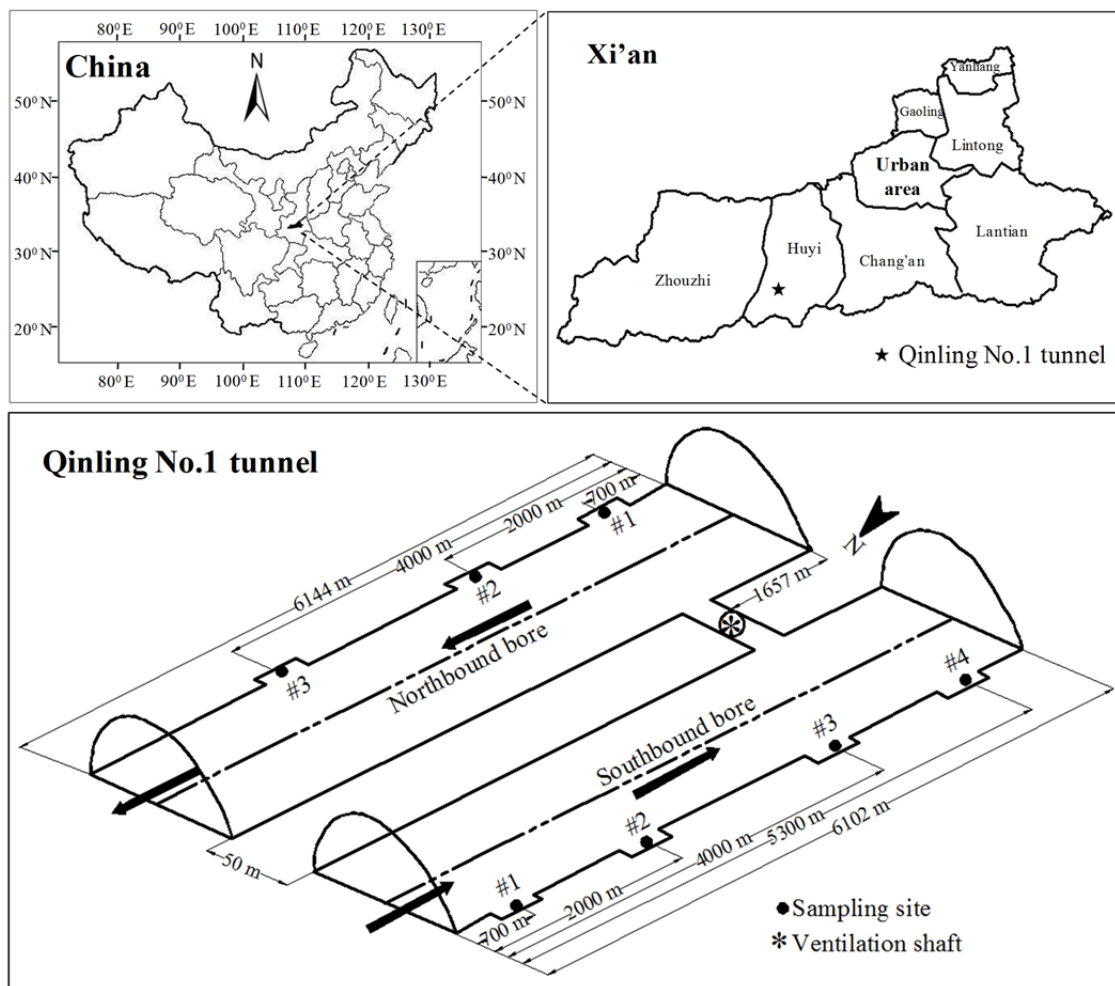


Fig. 1. Location of Qinling No. 1 Tunnel and its sketch map.

Sampling Method

The four-channel PM sampler (TH-16A, Tianhong Corporation, Wuhan, China) was used to sample inhalable particles (PM₁₀) and fine particles (PM_{2.5}) simultaneously. Two channels were loaded with 47-mm quartz-fiber filters, while the other two were loaded with 47-mm Teflon filters. The operating flow rate was 16.7 L min⁻¹, with a sampling height of 2 m. During this experiment, two samplers were used to collect PM concurrently, one of which was placed at Site #1, while the other one was moved day by day from Site #2 to Site #3, and then to Site #4. The duration of each sampling was 6–10 h to ensure that sufficient material was collected, with at least two sets of PM samples being collected at each site. The entire experiment lasted for one week (March 14–20, 2016), with 20 sampling sets being collected during two daily periods, one was at daytime between 8:00 to 20:00, and the other one was at nighttime between 20:00 to 8:00 (Table 1).

The meteorological parameters at each sampling site were recorded in parallel using an automatic weather station (GH-BPR, Huayun Puda Corporation, Beijing, China). A roadside laser traffic-survey instrument (AxleLight RLU11, NanoSense Corporation, Beijing, China) was used to investigate the traffic parameters during the entire test, including vehicle volume, speed and vehicle types.

Mass and Chemical Analysis

The PM mass concentrations were determined gravimetrically by weighing the filters before and after sampling (an MC5 Sartorius microbalance was used for weighing). Subsequently, the quartz-fiber filter was cut into two pieces to detect the carbonaceous species and water-soluble ions separately, whereas a Teflon filter was used to analyze the elements.

The contents of organic carbon (OC) and elemental carbon (EC) were determined by a Model-4 Semi-Continuous OC-EC Field Analyzer (Sunset Laboratory Inc.) with the thermal-optical transmission method (TOT; NIOSH, 2003). The water-soluble ions were analyzed by an ICS-5000 ion chromatograph (Thermo Fisher Scientific Inc.), following the method of Zhang *et al.* (2014). Trace elements were analyzed by an Epsilon-5 X-ray fluorescence spectrometer (PANalytical Inc.). Finally, three ionic species (NH₄⁺, NO₃⁻, and SO₄²⁻) and seventeen elements (Na, Mg, Al, P, S, K, Ca, Ti, Cr, Mn, Fe, Cu, Zn, Br, Ba, Hg, and Pb) were identified. More details of the analysis procedure are available in Section A2 in the supplementary material. The quality assurance and control of chemical analysis are

summarized in Section A3 in the supplementary material.

Statistical Analysis

Data analysis was performed using SPSS (Version 17). Species' correlation analysis was conducted based on Pearson correlation. Multivariate analysis of variance (multivariate-ANOVA) was carried out to test for significant variations in chemical composition between PM_{2.5} and PM₁₀ (Haase and Ellis, 1987). Moreover, the receptor modeling approach, including enrichment factor (EF) and principal component analysis (PCA), were adopted to identify the main sources of elements in the PM. Enrichment factor (EF) is a good indicator of the contributions of anthropogenic sources (Cevik *et al.*, 2009). It is calculated by the following equation:

$$EF_i = \frac{(C_i/C_r)_{Tunnel}}{(C_i/C_r)_{Background}} \quad (1)$$

where EF_i is the enrichment factor of element i , C_i is the concentration of element i , C_r is the concentration of the reference element, tunnel and background represent the sampling sources of the elements. Aluminum (Al) was selected as the reference element in this study (Sakan *et al.*, 2014), while the average background concentrations of elements in the soil of A Layer in Shaanxi Province were considered as the background values in this calculation (NEMCC, 1990).

PCA is a factor analysis method, which is a useful tool to apportion the emission sources and quantify their contributions (Larsen and Baker, 2003). In PCA, all factors with eigenvalues over 1 were extracted and rotated using the varimax method. Each of these factors can be identified as either an emission source or a chemical interaction. In order to determine the suitability of the dataset for PCA, a Kaiser-Meyer-Olkin (KMO) value of greater than 0.6 was required (Lawrence *et al.*, 2013). High values (close to 1) usually indicate that the PCA is useful with the selected dataset. Finally, the multifactorial analysis of variance (multifactorial-ANOVA) was applied to analyze the main influential factors on PM composition in the tunnel (Wolny and Kedzia, 2008).

RESULTS AND DISCUSSION

Chemical Composition of PM

The chemical compositions of PM_{2.5} and PM₁₀ were analyzed separately in this study. The results are summarized in Table 2. Moreover, the results of multivariate-ANOVA

Table 1. Summary of the samples in the tunnel.

Site	Bore	Sampling number	Sampling period
#1	Southbound	6	Daytime or Nighttime
#2		2	
#3		2	
#4		2	
#1	Northbound	4	
#2		2	
#3		2	

Table 2. Chemical compositions of PM in several studies (%).

City	Xi'an		Xining		Hong Kong		Guangzhou		Yantai	
	Year	Qinling No.1 Tunnel	2010	2010	2003	2003	2013	2013	2014	2014
Source	PM _{2.5}	PM ₁₀	Ambient air	Road dust	Shing Mun tunnel	Cheng Mun tunnel	Zhujiang tunnel	Wuzushan tunnel	Wuzushan tunnel	Kuixinglou tunnel
References	PM _{2.5}	PM ₁₀	Wang et al. (2015)	Han et al. (2014)	Cheng et al. (2010)	Cheng et al. (2010)	Dai et al. (2015)	Cui et al. (2016)	PM _{2.5} ^b	PM _{2.5} ^b
OC	34.10 ± 6.43	28.48 ± 16.02	13.04	5.98 ± 1.86	27.25	27.25	18.07	27.67	17.70	17.70
EC	11.96 ± 4.30	8.59 ± 3.81	4.70	0.60 ± 0.13	50.23	50.23	17.75	32.10	10.36	10.36
NH ₄ ⁺	3.19 ± 2.04	2.14 ± 1.54	5.82		2.14	2.14	0.18	0.87	0.14	0.14
NO ₃ ⁻	6.05 ± 4.42	4.30 ± 2.97	12.48	0.06 ± 0.06	0.84	0.84	0.11	3.28	3.65	3.65
SO ₄ ²⁻	8.98 ± 4.82	7.73 ± 4.40	16.20	1.38 ± 0.83	5.42	5.42	0.66	3.71	3.02	3.02
Na	1.48 ± 1.20	3.19 ± 2.67		0.84 ± 0.24	0.76	0.76	3.82	0.37	0.32	0.32
Mg	2.29 ± 1.27	4.17 ± 3.91		1.71 ± 0.39	0.27	0.27	0.54	2.01	1.13	1.13
Al	2.77 ± 1.57	3.67 ± 1.83		5.16 ± 0.62	0.17	0.17	3.41			
P	0.24 ± 0.14	0.26 ± 0.11		0.11 ± 0.03	0.05	0.05				
S	16.00 ± 7.64	12.89 ± 4.77			2.06	2.06				
K	0.48 ± 0.27	0.59 ± 0.24		1.55 ± 0.17	0.22	0.22	0.37	0.97	0.59	0.59
Ca	1.85 ± 1.27	4.27 ± 2.40		9.84 ± 2.33	0.42	0.42	2.09	5.42	2.12	2.12
Ti	0.04 ± 0.03	0.08 ± 0.04	0.07	0.26 ± 0.05	0.06	0.06		0.21	0.09	0.09
Cr	0.01 ± 0.01	0.02 ± 0.02		0.02 ± 0.01	0.01	0.01	0.01	0.01	0.14	0.14
Mn	0.03 ± 0.03	0.06 ± 0.04	0.07	0.08 ± 0.01	0.02	0.02	0.09	0.09	0.09	0.09
Fe	2.14 ± 1.86	3.56 ± 2.87	0.98	2.74 ± 0.49	0.73	0.73	4.23	4.59	4.19	4.19
Cu	0.02 ± 0.02	0.04 ± 0.03		0.03 ± 0.04	0.04	0.04	0.10	0.04	0.11	0.11
Zn	0.19 ± 0.04	0.26 ± 0.05	0.98	0.10 ± 0.08	0.15	0.15	0.17	0.17	0.17	0.17
Br	0.004 ± 0.004	0.003 ± 0.002			0.004	0.004				
Ba	0.14 ± 0.13	0.27 ± 0.23			0.06	0.06				
Hg	0.008 ± 0.005	0.011 ± 0.009								
Pb	0.03 ± 0.02	0.04 ± 0.02	0.21	0.03 ± 0.01	0.02	0.02	0.01	0.01	0.01	0.03

^a Mass fractions of each species were calculated based on the mass concentrations of PM_{2.5} and its corresponding species.

^b Mass fractions of each species were calculated based on the emission factors of PM_{2.5} and its corresponding species.

showed that the chemical compositions between PM_{2.5} and PM₁₀ were statistically distinct (the *p*-values from all the four tests, i.e., Pillai's trace, Wilk's lambda, Hotelling's trace, and Roy's largest root, were 0.001 less than 0.05). Moreover, EC and the elements of Na, Mg, Ca, Ti, Cu, Zn, and Ba were significantly influenced by particle size (Table 3). The mass fraction of EC in PM_{2.5} was higher than that in PM₁₀, whereas the fractions of Na, Mg, Ca, Ti, Cu, Zn, and Ba in PM_{2.5} were lower than those in PM₁₀.

OC and EC

The mass fractions of OC and EC in PM_{2.5} were 34.10 ± 6.43% (mean ± SD, *n* = 20) and 11.96 ± 4.30%, while their counterparts in PM₁₀ were 28.48 ± 16.02% and 8.59 ± 3.81%. The mass ratios of OC/EC in PM_{2.5} and PM₁₀ were 2.99 ± 1.11 and 3.30 ± 1.28, respectively, which showed that the contents of OC were noticeably higher than those of EC. EC is formed due to the incomplete combustion of fuel, and it can be emitted from motor vehicles directly. However, sources of OC are relatively complex, including the primary organic carbon (POC) directly emitted by motor vehicles and secondary organic carbon (SOC) produced from the gaseous precursors (Shen *et al.*, 2011). SOC generation is usually considered to occur when the mass ratio of OC/EC is greater than 2 (Deng *et al.*, 2013; Yu *et al.*, 2004). On the other hand, significant correlations were observed between OC and EC ($r_{PM_{2.5}} = 0.91$, $r_{PM_{10}} = 0.90$), suggesting a similar origin (i.e., direct emissions from motor vehicles) for both.

Water-Soluble Ions

The mass fractions of NH₄⁺, NO₃⁻, and SO₄²⁻ in PM_{2.5} were 3.19 ± 2.04% (*n* = 20), 6.05 ± 4.42%, and 8.98 ± 4.82%, while those in PM₁₀ were 2.14 ± 1.54%, 4.30 ± 2.97%, and 7.73 ± 4.40%. The order of the three ions in terms of their contents from highest to lowest was SO₄²⁻ > NO₃⁻ > NH₄⁺. Usually, NH₄⁺, NO₃⁻, and SO₄²⁻ can be called secondary ions, which are mainly derived from the gas-to-particle conversion of gaseous precursors (NH₃, NO_x, and SO₂), subsequently being coagulated in the PM in the form of (NH₄)₂SO₄, NH₄HSO₄, and NH₄NO₃ (Seinfeld and Pandis, 2016). In this study, NH₄⁺ was more strongly correlated with SO₄²⁻ ($r_{PM_{2.5}} = 0.95$, $r_{PM_{10}} = 0.91$) than NO₃⁻ ($r_{PM_{2.5}} = 0.72$, $r_{PM_{10}} = 0.70$). It is likely because the NH₄NO₃

is more easily volatilized into gas phase again due to its strong volatility (Chow, 1995). Moreover, it also indicated that the NH₄⁺ in the PM sampled in this tunnel was primarily in the form of (NH₄)₂SO₄ or NH₄HSO₄.

Elements

The elements can be classified into five groups (> 5%, 1–5%, 0.1–1%, 0.01–0.1%, and < 0.01%), in terms of their mass fractions (Table 4). It can be seen that the mass fraction of each element varied significantly. S was the most abundant element (16.00 ± 7.64% for PM_{2.5} and 12.89 ± 4.77% for PM₁₀, *n* = 20), followed by Al, Mg, Fe, Ca, and Na. These six elements accounted for 95.68% and 95.15% of the total mass of the 17 elements in PM_{2.5} and PM₁₀, respectively.

Elements can be categorized into metallic and non-metallic (Fig. 2). The non-metallic elements accounted for 58.59% and 39.42% of the total mass of the 17 elements in PM_{2.5} and PM₁₀, respectively, with S being the most abundant element. Meanwhile, the mass fractions of metallic elements were 41.41% and 60.58%, with Al, Mg, and Fe being the most abundant elements. Moreover, metallic elements can be further categorized into heavy and other metallic elements (Fig. 3). The heavy metallic element content was low, with contributions of 21.32% and 19.69% to the total mass of metallic elements in PM_{2.5} and PM₁₀, respectively. Fe was the most abundant element. Meanwhile, the mass fractions of other metallic elements were 78.68% and 80.31%, with Al, Mg, and Ca being the most abundant elements.

Source Identification

PM samples collected in the tunnel are a mixture derived from, but not limited to, vehicle exhaust, tire wear, brake wear, and resuspended road dust (Lawrence *et al.*, 2013). The origins of OC, EC, and secondary ions in the tunnel are known, based on past studies (Shen *et al.*, 2011; Seinfeld and Pandis, 2016). Therefore, this study emphasized the analysis of origins of the elements in the tunnel.

Application of Enrichment Factor (EF) Method

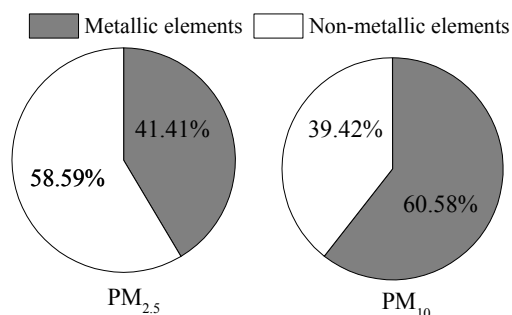
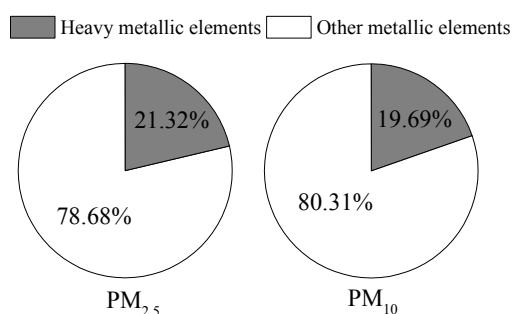
Fig. 4 shows the enrichment factors of 14 elements, except for Al, P, and S (P and S were not detected in the soil). The value of EF being equal to 10 is usually regarded as the criterion to determine whether an element is

Table 3. Analysis of the influence of particle size on PM composition.

Species	<i>F</i> -value	<i>p</i> -value	Species	<i>F</i> -value	<i>p</i> -value
OC	1.198	0.281	Ca	16.942	0.000
EC	6.904	0.012	Ti	16.160	0.000
NH ₄ ⁺	2.872	0.098	Cr	3.157	0.084
NO ₃ ⁻	0.036	0.851	Mn	3.896	0.056
SO ₄ ²⁻	1.535	0.223	Fe	3.919	0.055
Na	10.012	0.003	Cu	5.481	0.025
Mg	5.724	0.022	Zn	18.967	0.000
Al	2.925	0.095	Br	0.271	0.606
P	0.019	0.890	Ba	4.420	0.042
S	2.393	0.130	Hg	2.189	0.147
K	2.598	0.115	Pb	1.381	0.247

Table 4. Mass fraction distribution of elements.

Mass fraction	> 5%	1–5%	0.1–1%	0.01–0.1%	< 0.01%
PM _{2.5}	S	Al, Mg, Fe, Ca, Na	K, P, Zn, Ba	Ti, Pb, Mn, Cu, Cr	Hg, Br
PM ₁₀	S	Ca, Mg, Al, Fe, Na	K, Ba, P, Zn	Ti, Mn, Pb, Cu, Cr	Hg, Br

**Fig. 2.** Mass fractions of metallic and non-metallic elements (Metallic elements: Na, Mg, Al, K, Ca, Ti, Cr, Mn, Fe, Cu, Zn, Ba, Hg, and Pb; Non-metallic elements: P, S, and Br).**Fig. 3.** Mass fractions of heavy metallic and other metallic elements (Heavy metallic elements: Cr, Mn, Fe, Cu, Zn, Hg, and Pb; Other metallic elements: Na, Mg, Al, K, Ca, Ti, and Ba).

influenced by anthropogenic sources (Voutsas and Samara, 2002). $EF < 10$ indicates that the element is not enriched, mainly originating from natural sources (soil, crust, etc.), whereas $EF > 10$ implies that the element is significantly enriched, being greatly influenced by anthropogenic sources (i.e., motor vehicles in this study). It can be seen from Fig. 4 that Cu, Zn, Br, and Pb were enriched (EF values were between 10 and 100), while Hg was significantly enriched ($EF > 1000$). Therefore, these elements were mainly derived from traffic-related emissions in the tunnel. The EF values of Na, K, Ca, Ti, Mn, and Fe were less than 5, while the EF values of Mg, Cr, and Ba were between 5 and 10. Hence, the influence of anthropogenic sources was very weak on them. They mainly originated from natural sources in the tunnel, such as resuspended road dust.

Application of Principal Component Analysis (PCA)

The mass concentration of elements from PM_{2.5} and PM₁₀ were used for the PCA. The dataset provided KMO values of 0.652 for PM_{2.5} and 0.675 for PM₁₀, ensuring their suitability for PCA. In Table 5, three principal components with eigenvalues over 1 were extracted, which reflected specific elemental sources. All components explained 83.43% and 89.15% of the total variance in the dataset of PM_{2.5} and PM₁₀, respectively.

Component One showed the high loadings of Na, Mg, K, Ca, Ti, Cr, Mn, Fe, Cu, and Ba, with medium loading of Al. Usually, Mg, Al, and Ca are regarded as typical crustal elements (Tran *et al.*, 2012). Mg and Ca can also be derived from road surface wear (Kupiainen *et al.*, 2003). Nevertheless, the EF values of all these elements were lower than 10 (Fig. 4), which suggested that they mainly originated from resuspended road dust. Fe originates from crust, as well as brake wear (Sanders *et al.*, 2003). However, its EF values were lower than 10 (Fig. 4). Hence, its source was more likely to be resuspended road dust. Cu and Ba are the two main additives in brake pads (Sanders *et al.*, 2003; Birmili *et al.*, 2006). Furthermore, the EF values of Cu were greater than 10, which indicated that it was significantly influenced by the traffic flow in the tunnel. Therefore, Component One was strongly associated with a mixed source of resuspended road dust and brake wear.

Component Two was extracted based on the high loadings of P, S, and Zn, and medium loading of Hg. In addition, a high loading of Pb was observed in PM_{2.5} in Component Two, while medium loadings were observed in PM₁₀ in both Component One and Two. On the other hand, the correlation analysis results (Table 6) showed that only five elements had good correlations with EC emissions, including P, S, Zn, Hg, and Pb. Moreover, the EF values of

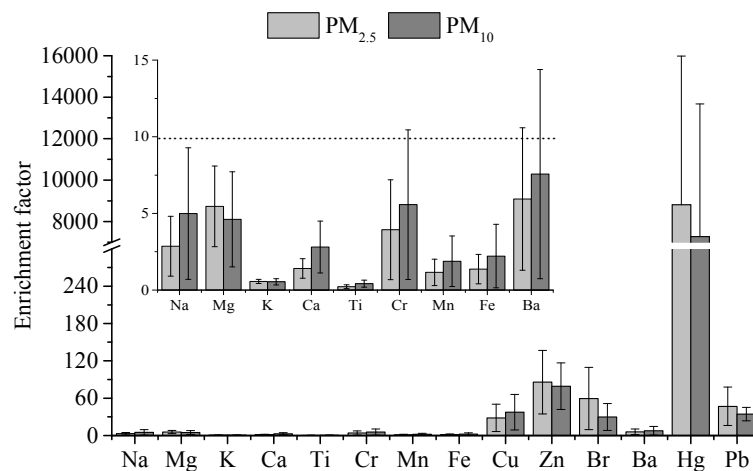


Fig. 4. Enrichment factors of elements in PM.

Table 5. Factor loadings of elements in the PCA (only loadings > 0.5 are shown).

Element	PM _{2.5}			PM ₁₀		
	Component 1	Component 2	Component 3	Component 1	Component 2	Component 3
Na	0.844			0.897		
Mg	0.772			0.941		
Al	0.516			0.599		
P		0.889			0.926	
S		0.919			0.970	
K	0.770			0.926		
Ca	0.908			0.944		
Ti	0.922			0.947		
Cr	0.971			0.986		
Mn	0.950			0.948		
Fe	0.982			0.985		
Cu	0.737			0.753		
Zn		0.910			0.841	
Br			0.884			0.951
Ba	0.917			0.978		
Hg		0.646			0.700	
Pb		0.836		0.660	0.533	
Variance (%)	46.77	26.62	10.04	56.61	24.20	8.34

Table 6. Correlation coefficients between elements and EC.

Element	EC		Element	EC	
	PM _{2.5}	PM ₁₀		PM _{2.5}	PM ₁₀
Na	-0.123	0.237	Mn	-0.129	-0.016
Mg	-0.150	0.022	Fe	-0.024	0.106
Al	0.237	0.425	Cu	0.378	0.473
P	0.733	0.902	Zn	0.723	0.866
S	0.555	0.897	Br	0.227	0.271
K	-0.210	0.310	Ba	0.198	0.069
Ca	0.151	0.310	Hg	0.555	0.506
Ti	0.155	0.274	Pb	0.562	0.637
Cr	-0.059	0.062			

Zn, Hg, and Pb were greater than 10 (Fig. 4). Hence, Pb was grouped into Component Two in this study. P is usually used as an additive in the lubricant oil (Alves *et al.*, 2015a). S is mainly generated by the combustion of sulfur-

bearing fuel (Lowenthal *et al.*, 1994). Zn is mostly present in rubber tires. Therefore, it is regarded as a product of tire wear (Degaffe and Turner, 2011). In addition, tailpipe can also emit a certain amount of Zn (Huang *et al.*, 1994).

Considering that EC is mainly derived from vehicle exhaust, with all the elements in Component Two being correlated with it, Component Two was attributed to a mixed source of vehicle exhaust and tire wear.

Component Three was interpreted as the exhaust emissions of diesel vehicles (DV), as it had the highest loading of Br. Br has been used as a marker for PM emissions from DV (Chow, 1995). Its EF values were greater than 10 (Fig. 4), which implied that it was clearly affected by the vehicles traveling through the tunnel.

Factors Influencing PM Profiles

Mobile source profiles of PM can be affected by a variety of factors, especially traffic conditions (Gillies *et al.*, 2001; Grieshop *et al.*, 2006; Nelson *et al.*, 2008). The traffic conditions in this study are illustrated in Fig. 5, including uphill/downhill, vehicle volume, speed, and fuel composition. Vehicle volumes at nighttime (227 veh h⁻¹) were significantly less than those at daytime (600 veh h⁻¹), as were the vehicle speeds (48.53 km h⁻¹ at nighttime and 55.60 km h⁻¹ at daytime). The reason was the difference in the fuel composition of vehicles during the two sampling periods. Vehicles were classified into two categories according to their fuel type, including diesel vehicles (DV: buses and trucks) and gasoline vehicles (GV: other vehicles such as passenger cars). There were more DV in the tunnel at nighttime (69.29% of DV at nighttime and 35.94% of DV at daytime), most of them being heavy-duty trucks, which moved slower than the GV under the same road conditions. Moreover, vehicle speeds during the test were around 50 km h⁻¹, which indicated that the traffic was free-flowing in the tunnel. Based on these traffic parameters collected in the tunnel, the running direction (i.e., southbound and northbound) reflected the differences in vehicle driving conditions (e.g., uphill/downhill and speed) synthetically, while the sampling period (i.e., daytime and nighttime) represented the discrepancies in vehicle fleet composition (e.g., vehicle volume and fuel type). Therefore, these two indexes were chosen as the influential variables. Their

impacts on the contents of PM species were analyzed by the multifactorial-ANOVA. Meanwhile, according to the previous PCA results (Table 5), the 17 elements were combined into three components for this analysis. Furthermore, three secondary ions (NH₄⁺, NO₃⁻, and SO₄²⁻) were combined into one component as well.

It can be seen from Table 7 that the PM species of OC, EC, and elements in Component One were strongly influenced by the running direction in the tunnel. The fractions of OC and EC in the southbound bore were both higher than those in the northbound bore (Figs. 6–7) due to the reverse slopes in two bores. The speed was reduced, while the engine torque was increased, when vehicles ascended through the southbound bore, which has a positive slope (+2.58%). Meanwhile, the fuel supply was increased to guarantee the engine's power, which induced poor fuel combustion and higher emissions of OC and EC. Nevertheless, the integrated contents of elements in Component One in the northbound bore were greater than those in the southbound bore (Fig. 8). Considering that these elements mainly originated from resuspended road dust and brake wear in the tunnel, it can be interpreted that more braking occurred when the vehicles descended through the northbound bore, which has a negative slope (-2.58%). Moreover, the vehicle speeds were slightly higher in the northbound bore during the same sampling period (Fig. 5). Therefore, more particles might be produced due to a stronger disturbance of the road dust.

Significant influence of the sampling period was observed on the contents of the elements in Component Three in PM_{2.5}, whereas its influence was not obvious in PM₁₀. The *p*-value (0.061) in PM₁₀ was very close to the significance level (0.05). Hence, this variable had some influence on the elements in Component Three. Only Br was grouped in Component Three, with the fractions of Br sampled at nighttime being higher than those collected at daytime (Fig. 9). Nevertheless, vehicle volumes at nighttime were significantly less than those at daytime (Fig. 5), which presented a reverse trend. Therefore, the influence of vehicle

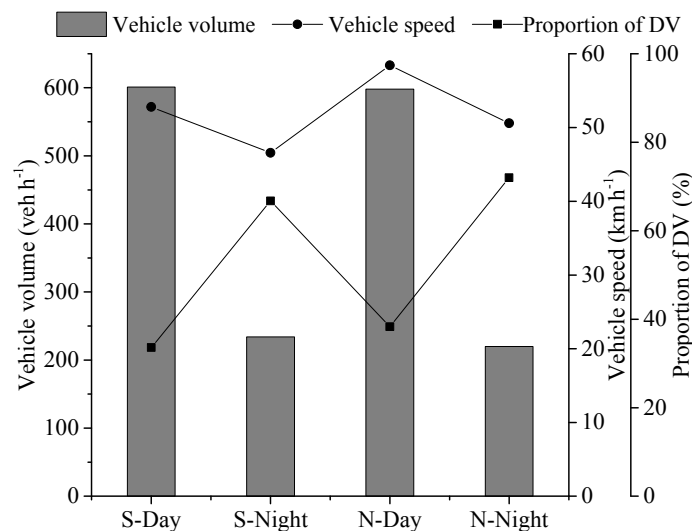
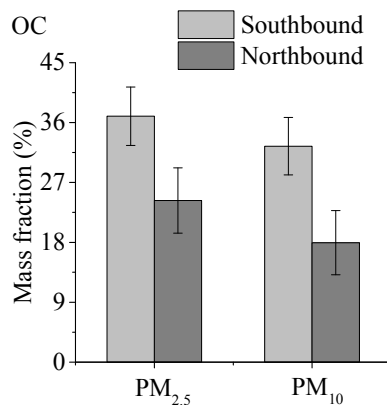
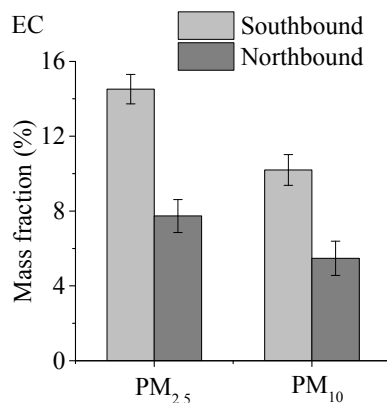
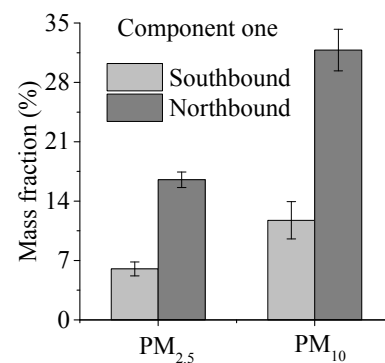
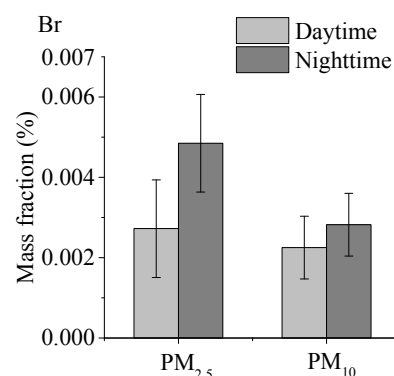


Fig. 5. Traffic conditions during the tunnel test (S: southbound, N: northbound, Day: daytime, Night: nighttime).

Table 7. Influence analysis of traffic conditions on PM profiles.

PM	Influential variables	OC		EC		Secondary ions	
		<i>F</i> -value	<i>p</i> -value	<i>F</i> -value	<i>p</i> -value	<i>F</i> -value	<i>p</i> -value
PM _{2.5}	Running direction	3.695	0.045	33.079	0.000	0.492	0.495
	Sampling period	0.001	0.973	0.036	0.853	0.009	0.927
	Running direction × Sampling period	0.012	0.913	0.673	0.426	0.493	0.494
PM ₁₀	Running direction	5.005	0.042	14.726	0.002	0.933	0.350
	Sampling period	0.156	0.699	1.001	0.334	0.011	0.919
	Running direction × Sampling period	0.290	0.599	1.971	0.182	0.542	0.474

PM	Influential variables	Elements					
		Component 1		Component 2		Component 3	
		<i>F</i> -value	<i>p</i> -value	<i>F</i> -value	<i>p</i> -value	<i>F</i> -value	<i>p</i> -value
PM _{2.5}	Running direction	73.103	0.000	1.063	0.320	0.180	0.678
	Sampling period	0.854	0.371	0.200	0.662	4.658	0.049
	Running direction × Sampling period	1.102	0.312	0.063	0.805	3.621	0.078
PM ₁₀	Running direction	37.034	0.000	0.429	0.523	0.225	0.642
	Sampling period	1.725	0.210	0.182	0.676	4.143	0.061
	Running direction × Sampling period	0.014	0.908	0.074	0.790	0.764	0.397

**Fig. 6.** Mass fractions of OC in the two directions.**Fig. 7.** Mass fractions of EC in the two directions.**Fig. 8.** Mass fractions of elements in Component One in the two directions. (Component One include elements of Na, Mg, Al, K, Ca, Ti, Cr, Mn, Fe, Cu, and Ba).**Fig. 9.** Mass fractions of Br during the two sampling periods.

volume on the Br content was very weak. Moreover, Br is primarily derived from tailpipe emissions of DV, and the proportions of DV at nighttime were significantly higher than those at daytime (Fig. 5). It can be concluded that the fuel composition in the tunnel was a major factor affecting the content of Br in the PM. In addition, the running direction and the sampling period did not have obvious

influences on the contents of secondary ions and elements in Component Two during this test (Table 7).

Comparison of PM Profiles

The mobile source profiles of PM were obtained with a mixed vehicle fleet in this study. The total mass of all the

detected constituents accounted for 92.00% and 84.60% of the total mass of PM_{2.5} and PM₁₀, respectively (Fig. 10). Carbonaceous species were the dominant constituent in the PM (46.06% for PM_{2.5} and 37.07% for PM₁₀), while the contents of OC were higher than those of EC. The mass fractions of elements were 27.73% for PM_{2.5} and 33.36% for PM₁₀. The non-metallic elements were the highest elements in PM_{2.5}, while the other metallic elements were the most abundant elements in PM₁₀. Moreover, the mass contributions of secondary ions were the lowest (18.22% for PM_{2.5} and 14.17% for PM₁₀).

Comparison with Other PM Sources

The source profiles of PM obtained in this study were compared with those from the other sources collected in northwestern China (Table 2), including ambient air (PM_{2.5} profile) and road dust (PM₁₀ profile; Han *et al.*, 2014; Wang *et al.*, 2015). The contents of OC and EC were significantly higher (2–14 times) than those from ambient air and road dust, which indicated that carbonaceous species were the primary markers of PM from vehicle emissions (Ancelet *et al.*, 2011; Pant *et al.*, 2017). Further, the mass fractions of three secondary ions were approximately 2 times lower than those from ambient air. A possible explanation for this difference was the weak illumination intensity in the tunnel, which partly limited the gas-to-particle conversion (Kang *et al.*, 2002; Lin *et al.*, 2010). The content of Fe was approximately 2 times higher than that from ambient air, which was similar to that from road dust. This implied that Fe primarily originated from the resuspended road dust in this tunnel. In addition, the fractions of P and Zn were up to 2 times higher than those from road dust, while the fractions of Cu and Pb were also slightly higher, indicating that these elements were influenced by passing vehicles, being highly enriched in the tunnel.

Comparison with Other Tunnel Studies

The PM_{2.5} profiles presented in this study were also compared with those from other tunnels in China (Table 2;

Cheng *et al.*, 2010; Dai *et al.*, 2015; Cui *et al.*, 2016). For the same species, the mass fractions presented in these tunnel tests were of the same order of magnitude. Meanwhile, considerable differences were also observed, depending on the differences in vehicle type, fuel type or quality, driving conditions, dust in the tunnel environment, etc. Therefore, local mobile source profiles need to be established.

The content of OC was higher (1.2–2.8 times) than those in the other tunnels, whereas the fraction of EC was similar to the values in the other tunnels, and very close to the value in the Kuixinglou tunnel. Moreover, the contents of the three secondary ions were also higher than those in the other tunnels. It can be attributed to the difference in sampling depths. Most of the sampling sites in this experiment were as deep as 2000 m inside the tunnel in the running direction (Fig. 1), whereas the maximum sampling depths were approximately 1000 m in the other tunnels. Hence, the secondary conversions of OC and ions in this experiment were significantly greater.

For the elements in Component One, the contents of Na, K, and Cr were within the range reported in the other tunnel studies. The fraction of Mg was close to the value in the Wuzushan tunnel. However, the elements of Ti and Cu were less than those in the other tunnels, and the elements of Al, Ca, Mn, and Fe were less than those in all other tunnels, except for the Shing Mun tunnel. These elements primarily originated from resuspended road dust and brake wear according to the previous PCA results. A probable reason was that, the vehicle volume during this tunnel test was less (411 veh h⁻¹ on average), with higher vehicle speed (51.84 km h⁻¹ on average), whereas a volume of more than 1000 veh h⁻¹ was recorded in the other tunnels, with an average speed of 33.40 km h⁻¹ in the Zhujiang tunnel. Heavy traffic flow and lower speed would cause frequent braking, leading to a stronger disturbance of the dust on the road surface.

With regard to the elements in Component Two, the contribution of Zn agreed well with the value reported in the other tunnel tests. The content of Pb was similar to the result in the Kuixinglou tunnel. While the fractions of P and S were higher (4–8 times) than the results from the Shing Mun tunnel, it was potentially due to the abundant phosphorus content in the lubricant oil and higher abundance of sulfur in the vehicle fuel during this tunnel test (Lowenthal *et al.*, 1994; Alves *et al.*, 2015a). In addition, the element of Br in Component Three was consistent with the result from Shing Mun tunnel.

CONCLUSIONS

PM_{2.5} and PM₁₀ samples were collected in the Qinling No. 1 Tunnel in Xi'an, China. A comprehensive snapshot of the chemical characteristics of the traffic-related PM emissions was generated that included OC, EC, three secondary ions (NH₄⁺, NO₃⁻, and SO₄²⁻), and 17 elements (Na, Mg, Al, P, S, K, Ca, Ti, Cr, Mn, Fe, Cu, Zn, Br, Ba, Hg, and Pb). On average, carbonaceous species were the most dominant constituents in the PM, forming mass

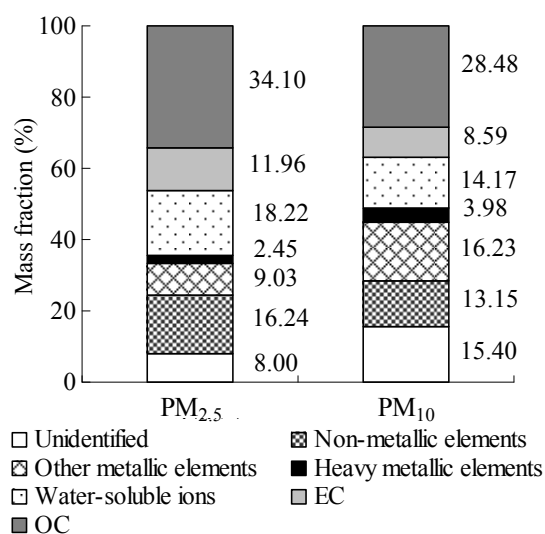


Fig. 10. Mass fractions of PM species in the tunnel.

contributions of 46.06% to the PM_{2.5} and 37.07% to the PM₁₀, with a higher content of OC than EC. The total mass fractions of the secondary ions were 18.22% for the PM_{2.5} and 14.17% for the PM₁₀, with SO₄²⁻ being the most abundant ion. Further, the summed mass of the 17 elements constituted 27.73% and 33.36% of the total mass of the PM_{2.5} and PM₁₀, respectively, with S being the most abundant element.

The sources of the different elements (i.e., exhaust and non-exhaust) in the PM were identified, and the 17 elements were grouped into 3 components by using PCA combined with EF. Component One comprised the elements Na, Mg, Al, K, Ca, Ti, Cr, Mn, Fe, Cu, and Ba, which were attributed to resuspended road dust and brake wear, whereas Component Two comprised the elements P, S, Zn, Hg, and Pb, which were attributed to vehicle exhaust and tire wear. Finally, Component Three contained only Br, which was mainly derived from the exhaust emissions of DV. Additionally, the emissions of OC, EC, and the elements in Component One were strongly influenced by vehicle driving conditions: The fractions of OC and EC increased with higher engine torque and poorer fuel combustion (when vehicles were ascending and moving at lower speeds), and the fraction of elements increased with frequent braking and the disturbance of road dust (when vehicles were descending and moving at higher speeds). Br, on the other hand, was mainly affected by the vehicle fleet composition, especially the fuel type, resulting in a higher fraction at nighttime because of the higher proportion of DV. However, the secondary ions and elements in Component Two were less influenced by these traffic parameters. Finally, based on a comparison between this study and other tunnel tests, the amount of measured OC and secondary ions may be affected by the sampling depth.

This is the first study to quantify PM profiles from mobile sources by using tunnel methodology in Xi'an in northwestern China. These results complement other studies conducted in various parts of China, improving our comprehension of PM pollution due to road traffic in this country.

ACKNOWLEDGEMENTS

This work was supported by the National Natural Science Foundation of China (No. 21607014, No. 51478045), the Foundation of Science and Technology Coordinating Innovative Engineering Projects of Shaanxi Province (No. 2016KTZDSF-02-01), and the Natural Science Basic Research Plan in Shaanxi Province of China (No. 2017JM7007).

SUPPLEMENTARY MATERIAL

Supplementary data associated with this article can be found in the online version at <http://www.aaqr.org>.

REFERENCES

Alves, C.A., Gomes, J., Nunes, T., Duarte, M., Calvo, A.,

- Custódio, D., Pio, C., Karanasiou, A. and Querol, X. (2015a). Size-segregated particulate matter and gaseous emissions from motor vehicles in a road tunnel. *Atmos. Res.* 153: 134–144.
- Alves, C.A., Barbosa, C., Rocha, S., Calvo, A., Nunes, T., Cerqueira, M., Pio, C., Karanasiou, A. and Querol, X. (2015b). Elements and polycyclic aromatic hydrocarbons in exhaust particles emitted by light-duty vehicles. *Environ. Sci. Pollut. Res. Int.* 22: 1–17.
- Alves, C.A., Oliveira, C., Martins, N., Mirante, F., Caseiro, A., Pio, C., Matos, M., Silva, H.F., Oliveira, C. and Camoes, F. (2016). Road tunnel, roadside, and urban background measurements of aliphatic compounds in size-segregated particulate matter. *Atmos. Res.* 168: 139–148.
- Ancelet, T., Davy, P.K., Trompetter, W.J., Markwitz, A. and Weatherburn, D.C. (2011). Carbonaceous aerosols in an urban tunnel. *Atmos. Environ.* 45: 4463–4469.
- Birmili, W., Allen, A.G., Bary, F. and Harrison, R.M. (2006). Trace metal concentrations and water solubility in size-fractionated atmospheric particles and influence of road traffic. *Environ. Sci. Technol.* 40: 1144–1153.
- Cevik, F., Goksu, M.Z.L., Derici, O.B. and Findik, O. (2009). An assessment of metal pollution in surface sediments of Seyhan dam by using enrichment factor, geoaccumulation index and statistical analyses. *Environ. Monit. Assess.* 152: 309–317.
- Cheng, Y., Lee, S.C., Ho, K.F., Chow, J.C., Watson, J.G., Louie, P.K.K., Cao, J.J. and Hai, X. (2010). Chemically speciated on-road PM_{2.5} motor vehicle emission factors in Hong Kong. *Sci. Total Environ.* 408: 1621–1627.
- Chiang, H.L. and Huang, Y.S. (2009). Particulate matter emissions from on-road vehicles in a freeway tunnel study. *Atmos. Environ.* 43: 4014–4022.
- Chow, J.C. (1995). Measurement methods to determine compliance with ambient air quality standards for suspended particles. *J. Air Waste Manage. Assoc.* 45: 320–382.
- Cui, M., Chen, Y.J., Tian, C.G., Zhang, F., Yan, C.Q. and Zheng, M. (2016). Chemical composition of PM_{2.5} from two tunnels with different vehicular fleet characteristics. *Sci. Total Environ.* 550: 123–132.
- Dai, S., Bi, X., Chan, L. Y., He, J., Wang, B., Wang, X., Peng, P., Sheng, G. and Fu, J. (2015). Chemical and stable carbon isotopic composition of PM_{2.5} from on-road vehicle emissions in the PRD region and implications for vehicle emission control policy. *Atmos. Chem. Phys.* 15: 3097–3108.
- Degaffe, F.S. and Turner, A. (2011). Leaching of zinc from tire wear particles under simulated estuarine conditions. *Chemosphere* 85: 738–743.
- Delfino, R.J., Staimer, N., Tjoa, T., Poldori, A., Arhami, M., Gillen, D.L., Kleinman, M.T., Vaziri, N.D., Longhurst, J., Zaldivar, F. and Sioutas, C. (2008). Circulating biomarkers of inflammation, antioxidant activity, and platelet activation are associated with primary combustion aerosols in subjects with coronary artery disease. *Environ. Health Perspect.* 116: 898–906.
- Deng, X.J., Wu, D., Yu, J.Z., Lau, A.K.H. and Li, F.

- (2013). Characterization of secondary aerosol and its extinction effects on visibility over the Pearl River Delta Region, China. *J. Air Waste Manage. Assoc.* 63: 1012–1021.
- Franco, V., Kousoulidou, M., Muntean, M., Ntziachristos, L., Hausberger, S. and Dilara, P. (2013). Road vehicle emission factors development: A review. *Atmos. Environ.* 70: 84–97.
- Gillies, J.A., Gertler, A.W., Sagebiel, J.C. and Dippel, W.A. (2001). On-road particulate matter (PM_{2.5} and PM₁₀) emissions in the Sepulveda Tunnel, Los Angeles, California. *Environ. Sci. Technol.* 35: 1054–1063.
- Grieshop, A.P., Lipsky, E.M., Pekney, N.J., Takahama, S. and Robinson, A.L. (2006). Fine particle emission factors from vehicles in a highway tunnel: Effects of fleet composition and season. *Atmos. Environ.* 40: 287–298.
- Haase, R.F. and Ellis, M.V. (1987). Multivariate analysis of variance. *J. Couns. Psychol.* 34: 404–413.
- Han, J.B., Han, B., Li, P.H., Kong, S.F., Bai, Z.P., Han, D.H., Dou, X.Y. and Zhao, X.D. (2014). Chemical characterizations of PM₁₀ profiles for major emission sources in Xining, northwestern China. *Aerosol Air Qual. Res.* 14: 1017–1027.
- Handler, M., Puls, C., Zbiral, J., Marr, I., Puxbaum, H. and Limbeck, A. (2008). Size and composition of particulate emissions from motor vehicles in the Kaisermuhlen-Tunnel, Vienna. *Atmos. Environ.* 42: 2173–2186.
- He, L.Y., Hu, M., Zhang, Y.H., Huang, X.F. and Yao, T.T. (2008). Fine particle emissions from on-road vehicles in the Zhujiang Tunnel, China. *Environ. Sci. Technol.* 42: 4461–4466.
- Ho, K.F., Ho, S.S.H., Lee, S.C., Cheng, Y., Chow, J.C., Watson, J.G., Louie, P.K.K. and Tian, L.W. (2009). Emissions of gas- and particle-phase polycyclic aromatic hydrocarbons (PAHs) in the Shing Mun Tunnel, Hong Kong. *Atmos. Environ.* 43: 6343–6351.
- Huang, X., Olmez, L., Aras, N.K. and Gordon, G.E. (1994). Emissions of trace elements from motor vehicles: Potential marker elements and source composition profile. *Atmos. Environ.* 28: 1385–1391.
- Huang, X.F., Yu, J.Z., He, L.Y. and Hu, M. (2006). Size distribution characteristics of elemental carbon emitted from Chinese vehicles: Results of a tunnel study and atmospheric implications. *Environ. Sci. Technol.* 40: 5355–5360.
- Kang, C., Han, J. and Sunwoo, Y. (2002). Hydrogen peroxide concentrations in the ambient air of Seoul, Korea. *Atmos. Environ.* 36: 5509–5516.
- Kupiainen, K.J., Tervahattu, H. and Räisänen, M. (2003). Experimental studies about the impact of traction sand on urban road dust composition. *Sci. Total Environ.* 308: 175–184.
- Larsen, R.K. and Baker, J.E. (2003). Source apportionment of polycyclic aromatic hydrocarbons in the urban atmosphere: A comparison of three methods. *Environ. Sci. Technol.* 37: 1873–1881.
- Lawrence, S., Sokhi, R., Ravindra, K., Mao, H.J., Prain, H.D. and Bull, I.D. (2013). Source apportionment of traffic emissions of particulate matter using tunnel measurements. *Atmos. Environ.* 77: 548–557.
- Lin, Y.C., Cheng, M.T., Lin, W.H., Lan, Y.Y. and Tsuang, B.J. (2010). Causes of the elevated nitrate aerosol levels during episodic days in Taichung urban area, Taiwan. *Atmos. Environ.* 44: 1632–1640.
- Liu, W.T., Ma, C.M., Liu, I.J., Han, B.C., Chuang, H.C. and Chuang, K.J. (2015a). Effects of commuting mode on air pollution exposure and cardiovascular health among young adults in Taipei, Taiwan. *Int. J. Hyg. Environ. Health* 218: 319–323.
- Liu, Y., Gao, Y., Yu, N., Zhang, C.K., Wang, S.Y., Ma, L.M., Zhao, J.F. and Lohmann, R. (2015b). Particulate matter, gaseous and particulate polycyclic aromatic hydrocarbons (PAHs) in an urban traffic tunnel of China: Emission from on-road vehicles and gas-particle partitioning. *Chemosphere* 134: 52–59.
- Liu, Y., Wang, S.Y., Lohmann, R., Yu, N., Zhang, C.K., Gao, Y., Zhao, J.F. and Ma, L.M. (2015c). Source apportionment of gaseous and particulate PAHs from traffic emission using tunnel measurements in Shanghai, China. *Atmos. Environ.* 107: 129–136.
- Lowenthal, D.H., Zielinska, B., Chow, J.C., Watson, J.G., Gautam, M., Ferguson, D.H., Neuroth, G.R. and Stevens, K.D. (1994). Characterization of heavy-duty diesel vehicle emissions. *Atmos. Environ.* 28: 731–743.
- MEPC (Ministry of Environmental Protection of the People's Republic of China (2018). China vehicle environmental management annual report. http://www.zhb.gov.cn/gkml/hbb/qt/201706/t20170603_415265.htm, Last Access: 2 February 2018.
- Na, K., Biswas, S., Robertson, W., Sahay, K., Okamoto, R., Mitchell, A. and Lemieux, S. (2015). Impact of biodiesel and renewable diesel on emissions of regulated pollutants and greenhouse gases on a 2000 heavy duty diesel truck. *Atmos. Environ.* 107: 307–314.
- NEMCC (National Environmental Monitoring Center of China) (1990). *Chinese soil element background content*. Chinese Environment Science Press, Beijing, China.
- Nelson, P.F., Tibbett, A.R. and Day, S.J. (2008). Effects of vehicle type and fuel quality on real world toxic emissions from diesel vehicles. *Atmos. Environ.* 42: 5291–303.
- NIOSH (2003). Manual of analytical methods (NMAM). In *Monitoring of diesel particulate exhaust in the workplace, Chapter Q, Third supplement to NMAM*, 4 ed., O'Connor, P.F. and Schlecht, P.C. (Eds.), NIOSH, Cincinnati, OH. DHHS (NIOSH) Publication No. 2003-154.
- Pant, P., Shi, Z.B., Pope, F.D. and Harrison, R.M. (2017). Characterization of traffic-related particulate matter emissions in a road tunnel in Birmingham, UK: Trace metals and organic molecular markers. *Aerosol Air Qual. Res.* 17: 117–130.
- Pietikainen, M., Valiheikki, A., Oravisjarvi, K., Kolli, T., Huuhtanen, M., Niemi, S., Virtanen, S., Karhu, T. and Keiski, R.L. (2015). Particle and NO_x emissions of a non-road diesel engine with an SCR unit: The effect of fuel. *Renew. Energy* 77: 377–385.
- Pio, C., Mirante, F., Oliveira, C., Matos, M., Caseiro, A.,

- Oliveira, C., Querol, X., Alves, C., Martins, N. and Cerqueira, M. (2013). Size-segregated chemical composition of aerosol emissions in an urban road tunnel in Portugal. *Atmos. Environ.* 71: 15–25.
- Sakan, S.M., Dević, G.J., Relić, D.J., Anđelković, I.B., Sakan, N.M. and Dorđević, D.S. (2014). Environmental assessment of heavy metal pollution in freshwater sediment, Serbia. *Clean-Soil Air Water* 43: 838–845.
- Sanders, P.G., Xu, N., Dalka, T.M. and Maricq, M.M. (2003). Airborne brake wear debris: Size distribution, composition, and a comparison of dynamometer and vehicle tests. *Environ. Sci. Technol.* 37: 4060–4069.
- Seinfeld, J.H. and Pandis, S.N. (2016). *Atmospheric chemistry and physics: From air pollution to climate change*. John Wiley & Sons, Inc., Hoboken, USA.
- Shen, Z.X., Cao, J.J., Liu, S.X., Zhu, C.S., Wang, X., Zhang, T., Xu, H.M. and Hu, T.F. (2011). Chemical composition of PM₁₀ and PM_{2.5} collected at ground level and 100 meters during a strong winter-time pollution episode in Xi'an, China. *J. Air Waste Manage. Assoc.* 61: 1150–1159.
- Spira-Cohen, A., Chen, L.C., Kendall, M., Lall, R. and Thurston, G.D. (2011). Personal exposures to traffic-related air pollution and acute respiratory health among Bronx schoolchildren with asthma. *Environ. Health Perspect.* 119: 559–565.
- Thorpe, A. and Harrison, R.M. (2008). Sources and properties of non-exhaust particulate matter from road traffic: A review. *Sci. Total Environ.* 400: 270–282.
- Tran, D.T., Alleman, L.Y., Coddeville, P. and Galloo, J.C. (2012). Elemental characterization and source identification of size resolved atmospheric particles in French classrooms. *Atmos. Environ.* 54: 250–259.
- Voutsas, D. and Samara, C. (2002). Labile and bioaccessible fractions of heavy metals in the airborne particulate matter from urban and industrial areas. *Atmos. Environ.* 36: 3583–3590.
- Wang, P., Cao, J.J., Shen, Z.X., Han, Y.M., Lee, S.C., Huang, Y., Zhu, C.S., Wang, Q.Y., Xu, H.M. and Huang, R.J. (2015). Spatial and seasonal variations of PM_{2.5} mass and species during 2010 in Xi'an, China. *Sci. Total Environ.* 508: 477–487.
- Wolny, S. and Kedzia, J. (2008). Application of multifactorial variance analysis for assessment of temperature influence on selected parameters of recovery voltage of paper-oil insulation. *Przegląd Elektrotechniczny* 84: 218–221.
- Yao, Z.L., Shen, X.B., Ye, Y., Cao, X.Y., Jiang, X., Zhang, Y.Z. and He, K.B. (2015). On-road emission characteristics of VOCs from diesel trucks in Beijing, China. *Atmos. Environ.* 103: 87–93.
- Yu, S., Dennis, R.L., Bhave, P.V. and Eder, B.K. (2004). Primary and secondary organic aerosols over the United States: Estimates on the basis of observed organic carbon (OC) and elemental carbon (EC), and air quality modeled primary OC/EC ratios. *Atmos. Environ.* 38: 5257–5268.
- Zhang, F., Chen, Y.J., Tian, C.G., Wang, X.P., Huang, G.P., Fang, Y. and Zong, Z. (2014). Identification and quantification of shipping emissions in Bohai Rim, China. *Sci. Total Environ.* S 497–498: 570–577.
- Zhang, Y.Z., Yao, Z.L., Shen, X.B., Liu, H. and He, K.B. (2015a). Chemical characterization of PM_{2.5} emitted from on-road heavy-duty diesel trucks in China. *Atmos. Environ.* 122: 885–891.
- Zhang, Y.L., Wang, X.M., Li, G.H., Yang, W.Q. and Huang, Z.H. (2015b). Emission factors of fine particles, carbonaceous aerosols and traces gases from road vehicles: Recent tests in an urban tunnel in the Pearl River Delta, China. *Atmos. Environ.* 122: 876–884.
- Zhao, Q., Yu, Q. and Chen, L.M. (2010). Particulate matter and particle-bound polycyclic aromatic hydrocarbons in the Dapu road tunnel in Shanghai. *Int. J. Environ. Pollut.* 41: 21–37.

Received for review, April 13, 2018

Revised, July 6, 2018

Accepted, September 17, 2018